Frontiers in Computing and Intelligent Systems
ISSN: 2832-6024 | Vol. 9, No. 2, 2024

Solar Radiometer Efficiency Study Based on Particle Swarm Optimization Algorithms and Variable Parameter Goal Planning Design Models

Jiaxuan Xie *, Wenjie Zhou

College of Physics and Electronic Information Engineering, Guilin University of Technology, Guilin, Guangxi, China
*** Corresponding author:** Jiaxuan Xie

Abstract: Sunset mirror is an important basic light collection unit in a tower photovoltaic power generation system, and the construction of sunset mirrors as optical power generation is of great significance for building green ecological targets in China. Based on the planning of establishing a heliostat field in a circular area, a shading efficiency model is established to study the optical efficiency of the heliostat field and its output efficiency under different sunlight angles and mirror parameters. Then, based on the theoretical algorithm of shading efficiency, the parameter information of the heliostat field is optimized, and the optimal solution of the design parameters of the heliostat field satisfying the constraints is solved by using the optimized particle swarm algorithm. This research can make fuller use of solar energy resources and achieve the goals of sustainable development and environmental protection.

Keywords: Optical Efficiency Theoretical Algorithms; Shadow Shading Efficiency Models; Variable Parameter Target Planning; Particle Swarm Optimization.

1. Introduction

Since the 21st century, traditional fossil energy and environmental problems have become more and more prominent, and the development of clean and efficient new energy sources has become a project strongly supported by various countries. Considering a circular area of heliostat field, the absorber tower is built in the center of the circular heliostat field with an installation height of 4m, and the environmental parameters such as solar altitude angle, azimuth angle, and normal direct radiant illuminance (see Figure 1), the environmental parameters of the local time node are calculated according to the given spatial coordinates of the heliostats, and the theoretical model of the shadowing blocking efficiency is set up, and the shading loss of any two heliostats is deduced from the coordinates points.

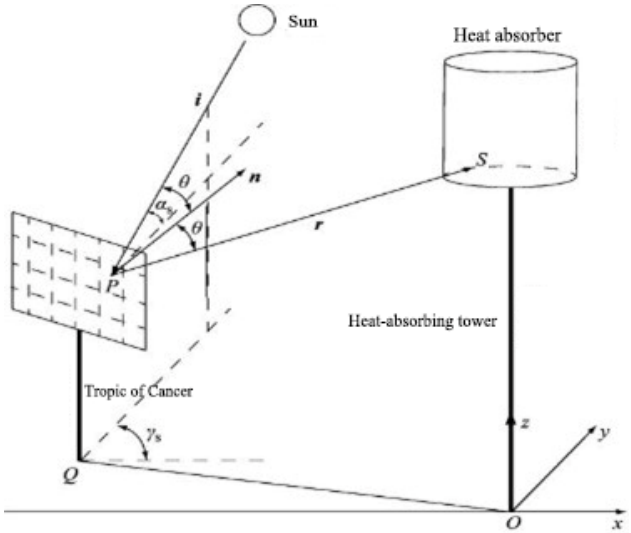

Figure 1. Example diagram of solar altitude angle parameter (Figure Source Literature) [1-2]

Secondly, the optical efficiency parameters of the heliostat field are calculated by the established theoretical model of light-blocking efficiency, and then the average output thermal power of heliostat mirrors per unit area of the mirror surface is solved, and then the objective planning of variable parameters of the heliostat field is calculated, and the multivariate nonlinear objective planning model is established, and the globally optimal solution of the heliostat parameters is realized based on the optimized particle swarm algorithm after the set rated power is solved.

2. Study of the Output Thermal Power of Heliostats Based on a Theoretical Model of Shadow-Blocking Light Efficiency

2.1. Solving for Solar Parameters

In the process of considering the average optical efficiency of the mirror heliographic field, the rotation and revolution of the Earth may cause real-time variations in the direct radiance of the sunlight-projecting mirror heliographic field, which is represented by the solar position through the solar altitude angle and azimuthal angle.

The center of the circular fixed-sun field is located at 98.5°E longitude and 39.4°N latitude, with an altitude of 3000m and a construction radius of 350m, where φ is the local dimension of +39.4°:

$$\omega = \frac{\pi}{12}(ST - 12) \tag{1}$$

Where ST is the local time and ω is the solar time. Approximate formula for normal direct radiation irradiance DNI is:

$$
\begin{aligned}
DNI &= G_0[a + be^{-\frac{c}{\sin\alpha_s}}] \\
a &= 0.4237 - 0.00821(6-H)^2 \\
b &= 0.5055 + 0.00595(6.5-H)^2 \\
c &= 0.2711 + 0.01858(2.5-H)^2
\end{aligned} \tag{2}
$$

Where G_0 is the solar constant which takes the value of 1.366kW/m2, H is the altitude of 3km.

The variation of DNI with time is shown in Figure 2.

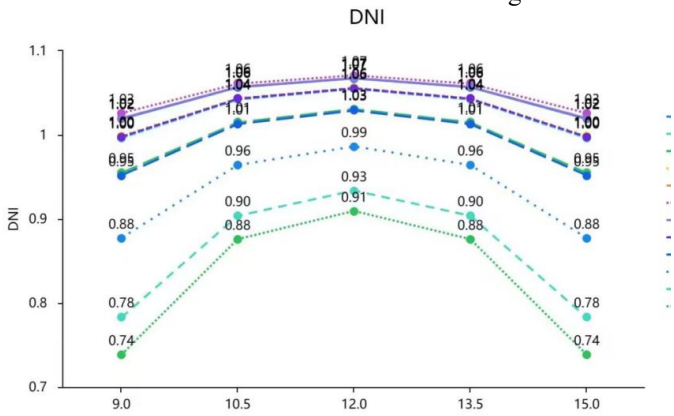

Figure 2. Statistical graph of DNI over time

2.2. The Determination of the Number of Network Layers

Take any fixed-sun mirror (denote it as n) and establish the coordinate system as shown in the figure by combining the above incident and reflected rays from the sun.

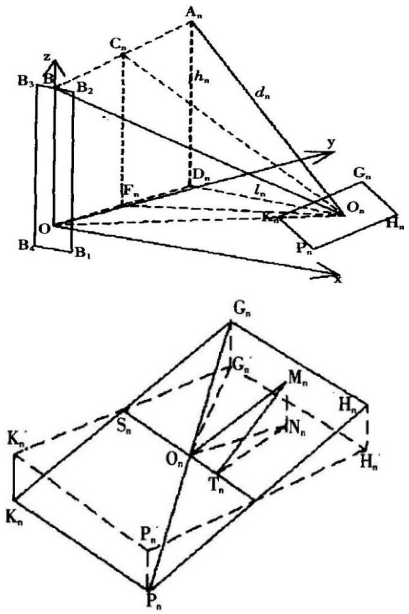

Figure 3. Establishment of the coordinate system of the heliostat and the projection diagram of each point

Where the collector tower bottom center coordinates are (0,0,0), the centers of the heliostat are in the plane of $z = 4$. $B1, B2, B3, B4$ in the $x-z$ plane on behalf of the tower, the collector tower tower width parameter is L_τ; G_n, H_n, P_n, K_n were set to represent the four angular points of the heliostat, O_n for the center of the mirror of the heliostat n, the coordinates of which are $(x_n, y_n, 4)$.) [3-4].The coordinates of the four corner points of the fixed heliograph are

$G_n(x_{gn}, y_{gn}, z_{gn})$, $H_n(x_{hn}, y_{hn}, z_{hn})$, $P_n(x_{pn}, y_{pn}, z_{pn})$, and $K_n(x_{kn}, y_{kn}, z_{kn})$

Express the angle between the fixed heliograph and the $x-y$ plane in terms of (0 ≤< 90°), and combine this with the geometric relationship in Figure 3 to obtain:

$$
\cos\mu_n = \frac{d_n \sin\alpha_s + H_1}{2 \cdot d_n \cos\theta_n} \tag{3}
$$

Where, d_n - the distance from the center point O_n of the heliostat mirror to the center point B of the collector entrance at the top of the tower, $d_n = \sqrt{H_1^2 + x_n^2 + y_n^2}$; Ht - the height coordinates of the target point, i.e., the difference in height between the point B and the point O_n; θ_n - the angle of incidence or reflection of the light rays on the mirror surface; αs - the sun's altitude angle [5].

The counterclockwise angle between the horizontal straight line S_nO_n passing through the mirror center point $O_n(x_n, y_n, 4)$on the heliostat mirror and the positive direction of the y-axis is the angle of intersection between the heliostat mirror and the $y-z$ plane, which is denoted by ρn, and varies within the range of $[0, \pi]$, and is obtained by combining the geometrical relations in Figure 3:

$$
\begin{aligned}
\left|O_nF_n\right| &= \sqrt{\left(x_n - \frac{1}{2}x_n\right)^2 + \left(y_n - \frac{1}{2}y_n\right)^2} \\
\sin\varphi_n &= \frac{x_n - \frac{1}{2}x_n'}{\left|O_nF_n\right|}
\end{aligned} \tag{4}
$$

Where φ_n - the angle between the projection of the normal of the heliostat in the $x-y$ plane and the positive semi-axis of the y-axis.

At a certain moment the angle between the heliostat and the $y-z$ plane is shown below:

$$
\rho_n = \phi_n + \frac{1}{2}\pi \tag{5}
$$

From this, the coordinates of the 4 vertices of the fixed-sun mirror

$G_n(x_{gn}, y_{gn}, z_{gn})$, $H_n(x_{hn}, y_{hn}, z_{hn})$, $P_n(x_{pn}, y_{pn}, z_{pn})$, and $K_n(x_{kn}, y_{kn}, z_{kn})$ are calculated.

Take any fixed-sun mirror n's mirror surface is divided into a number of micro-elements, using the above model center coordinates (x_{mn}, y_{mn}, z_{mn}), substituting the above model to solve the micro-element dsnk thrown into the micro-element ds'nk and the receiving tower is located in the plane of the micro-element $ds'nk$, whose corresponding coordinates $(x'_{mn}, y'_{mn}, z'_{mn})$, the microelement ds'_{jk} $(x'_{mj}, y'_{mj}, z'_{mj})$ through which the incident light of the microelement dsnk and the reflected light intersect with the plane in which the mirror of one of the other fixed-heaven mirrors j is located, respectively. z'_{mj} , ds''_{jk} $(x''_{mj}, y''_{mj}, z''_{mj})$.

The total effectively utilized area of the incident light received by the heliostat η is obtained by accumulating all the microelements $dsnk$ on the heliostat n that are able to receive the incident light, and the effective utilization rate of the heliostat n to receive the incident light from the sun is [4]:

$$\eta_{sn} = \frac{2 \cdot K_s \cdot d_s}{DM^2 \sin 2\beta_n} \tag{6}$$

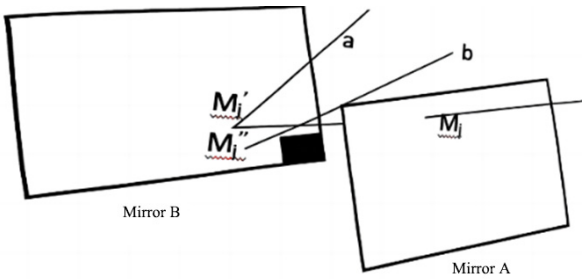

Figure 4. Microelement diagram of the theoretical model of shaded light-blocking efficiency

Where K_s - the total number of microelements capable of receiving incident light.

Similarly, all the microelements $dsnk$ on the heliostat n that are able to reflect the light projected light projected into the collector are accumulated to give the total effectively utilized area of the heliostat n reflecting the sunlight to give the effective utilization rate of the heliostat η reflecting the sunlight into the collector as:

$$\eta_{bn} = \frac{2 \cdot K_b \cdot d_s}{DM^2 \sin 2\beta_n} \tag{7}$$

Where, K_b - the total number of microelements capable of reflecting sunlight into the collector; dsn - the area of equal microelements on the mirror surface of the heliostat mirror η.

In summary, the total effective utilization rate of the heliostat mirror η is:

$$\eta_{sbn} = \eta_{sn} \times \eta_{bn} \tag{8}$$

The average annual optical efficiency can be calculated with the help of the MATLAB program.

2.3. Mathematical Modeling and Solution of Cosine Efficiency

Cosine is the most serious part of the optical efficiency loss. Cosine efficiency characterizes the mirror surface of the actual size of the light-gathering area. As shown in the Figure 5 for the cosine efficiency diagram, its value is equal to the actual lighting area of the mirror and the mirror area ratio, the smaller the angle value, the higher the cosine efficiency, and vice versa [6].

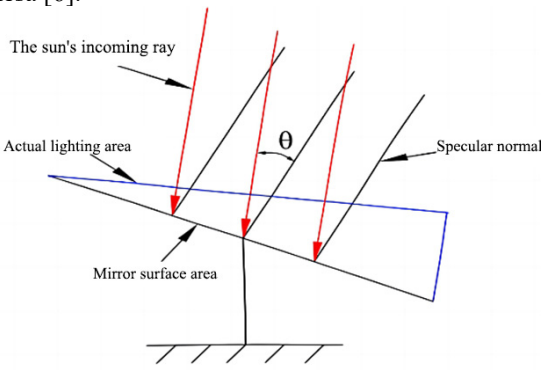

Figure 5. Cosine efficiency diagram

Fixed sun mirror center point $O_n\ (x_n, y_n, 4)$, the collector center point coordinates for (0, 0,80), s for the sun incident light unit vector, n for the mirror surface normal unit vector. From the above modeled law of reflection of light rays, the angle of incidence on the mirror of a fixed-sun mirror is equal to the angle of reflection, which can be obtained by combining the geometric vector equations:

$$\eta_{\cos} = \cos\theta = \left|\frac{1+\cos(2\theta)}{2}\right| = \left|\sqrt{\frac{1-\vec{s}\cdot\vec{r}}{2}}\right| \tag{9}$$

Where:

$$s = (-\cos\alpha_s \sin\gamma_s, -\cos\alpha_s \cos\gamma_s, -\sin\alpha_s) \tag{10}$$

$$r = \frac{(-x,-y,H-z)}{\sqrt{x^2+y^2+(H-z)^2}} \tag{11}$$

Substituting the solar altitude angle parameter, combined with the geometric relationship between the light projection of the heliostat, the average cosine efficiency can be calculated as follows.

2.4. Truncation Efficiency and Atmospheric Transmittance Calculations

In the output power of heliostat field, the truncation efficiency is an important part of its optical efficiency [7]. Using the HFCAL model [8], a circular Gaussian distribution is utilized to calculate the heat flow density function on the collector surface, and the energy flow density $Q(x_R, y_R)$ at any point (x_R, y_R) on the surface of the collector for any heliostat n as well as the spot thermal power $Q_{rec.in}$, the heliostat truncation efficiency is:

$$\eta_{trunc} = \frac{1}{2\pi\sigma_{tot}^2} \iint_{x_R y_R} e^{\left(-\frac{(x_R-x_a)^2+(y_R-y_a)^2}{2\sigma_{tot}^2}\right)} dy_R dx_R \tag{12}$$

$$\sigma_{tot} = \sqrt{d_{HR}^2(\sigma_{sun}^2 + \sigma_{bq}^2 + \sigma_{ast}^2 + \sigma_{track}^2)} \tag{13}$$

Where σ_{sun} is the standard deviation of the sun shape; σ_{bq} is the standard deviation of the beam quality error; σ track is the standard deviation of the tracking error, and σ_{ast} is the standard deviation of the image dispersion error, where:

$$\sigma_{bq}^2 = (2\sigma_s)^2 \tag{14}$$

$$H_t = \sqrt{SH \times SW}\left|\frac{d}{f} - \cos\theta\right|,\quad W_s = \sqrt{SH \times SW}\left|\frac{d}{f}\cos\theta - 1\right| \tag{15}$$

Where σ_s is the standard deviation of the slope error; H_t and W_s are the dimensions of the spot on the collector in the meridional and arc-vector directions; SH and SW are the height (80 m) and width of the heliostat; and f is the axial focal length of the heliostat.Where the atmospheric transmittance $\eta_{at} = 0.99321 - 0.0001176 d_{HR} + 1.97 * 10 - 8 * d_{HR}^2$ $(d_{HR} \leq 1000)$ [9], and calculate the linear distance d_{HR} between any heliostat n and the collector.

2.5. Average Optical Efficiency and Output Power Solution

Based on the above model modeling and parameter solving, the optical efficiency η of any certain heliostat η is:

$$\eta_n = \eta_{sb}\eta_{\cos}\eta_{at}\eta_{trunc}\eta_{ref} \tag{16}$$

The output thermal power formula for a fixed heliostat is calculated under the given heliostat field parameters as:

$$E_{field} = DNI \cdot \sum_{i}^{N} A_i\eta_i \tag{17}$$

The average output thermal power W_a per unit area of mirror is calculated as:

$$W_a = \frac{E_{field}}{S \cdot N} \tag{18}$$

The average optical efficiency and output power can be obtained by solving using MATLAB by substituting the obtained parameters

3. Multivariate Non-linear Objective Planning Models based on Variable-Parameter Objective Planning

3.1. Construction of Variable Parameter Target Planning

The rated annual average thermal power output of the fixed sunglasses field is 60 MW, the bottom of the heat collection tower for the center of the coordinates of the origin, due east for the x-axis, due north for the y-axis, perpendicular to the ground upwards for the z-axis to establish the spatial coordinates system. Based on the theoretical model establishment of shadow blocking light efficiency, the annual average output thermal power is calculated.

$$E_{field} = DNI \cdot \sum_{i}^{N} A_i\eta_i \tag{19}$$

3.2. Multi-objective Linear Programming Modeling

Set the positive and negative bias parameter variables. Let $f_i(i = 1,2,\dots,l)$ the ith parameter objective function, its positive deviation variable $d+i = \max\{f_i - d_i^0, 0\}$ indicates the part of the decision value that exceeds the target value, and the negative deviation parameter variable $d - i = -max\{f_i - d_i^0, 0\}$ $i$ndicates the part of the decision value that does not reach the target value, and here d0i indicates the target value of f_i. Because the decision value can not both exceed the target value at the same time for reaching the target value, i.e., constant $d_i^+ * d_i^- = 0$. The coordinate calculations are all absolutely rigid constraints, and the distance between the centres of the bases of neighbouring heliostats in the design of the heliostat field parameter is a first-order priority factor, and any heliostat xoy-plane coordinate restriction region is [100,350].

This objective planning involves several variable parametric quantities, and solving for the first level objective under the first level priority factor condition, i.e., solving the following linear plan:

$$\begin{cases} \min \mathrm{d}_1^- - \mathrm{d}_1^+ \\ \text{s.t.} \begin{cases} H_t = \sqrt{SH \times SW}\left|\dfrac{d}{f} - \cos\theta\right| + \mathrm{d}_1^- - \mathrm{d}_1^+ \\ W_s = \sqrt{SH \times SW}\left|\dfrac{d}{f}\cos\theta - 1\right| + \mathrm{d}_2^- - \mathrm{d}_2^+ \\ \sigma_{ast} = \sqrt{\dfrac{0.5(H_t^2 + W_s^2)}{4d}} + \mathrm{d}_3^- - \mathrm{d}_3^+ \end{cases} \\ \mathrm{d}_i^-,\ \mathrm{d}_i^+ \geq 0,\ \mathrm{i} = 1,2,3,4 \end{cases} \tag{20}$$

To find the second level objective, i.e., to solve the following linear programme.

$$\begin{cases} \min \mathrm{d}_4^- - \mathrm{d}_4^+ + \mathrm{d}_5^- - \mathrm{d}_5^+ \\ \text{s.t.} \begin{cases} \eta_{trunc} = \dfrac{1}{2\pi\sigma_{tot}^2}\iint_{x_{mn}y_{mn}} e^{\left(-\frac{(x_R - x_a)^2 + (y_R - y_a)^2}{2\sigma_{tot}^2}\right)} dy_{mn}dx_{mn} + \mathrm{d}_4^- - \mathrm{d}_4^+ \\ Q_{rec,in} = \dfrac{P_m}{2\pi\sigma_{tot}^2}\iint_{x_{mn}y_{mn}} e^{\frac{(x_{mn} - x_{mn})^2 + (y_{mn} - y_{mn})^2}{2\sigma_{tot}^2}} dy_{mn}dx_{mn} + \mathrm{d}_5^- - \mathrm{d}_5^+ \end{cases} \\ \mathrm{d}_i^-,\ \mathrm{d}_i^+ \geq 0,\ \mathrm{i} = 4,5,6,7 \end{cases} \tag{21}$$

Find the third level objective, i.e., solve the following linear programming.

$$\begin{cases} \min\ d_8^- - d_8^+ \\ \text{s.t.} \begin{cases} \eta_{sn} = \dfrac{2 \cdot K_s \cdot d_s}{DM^2 \sin 2\beta_n} + \mathrm{d}_6^- - \mathrm{d}_6^+ \\ \eta_{bn} = \dfrac{2 \cdot K_b \cdot d_s}{DM^2 \sin 2\beta_n} + \mathrm{d}_7^- - \mathrm{d}_7^+ \\ \eta_{at} = 0.99321 - 0.0001176 d_{HR} + 1.97 \times 10^{-8} \times d_{HR}^2 \\ \eta_{\cos} = \left|\dfrac{1 + \cos(2\theta)}{2}\right| + \mathrm{d}_8^- - \mathrm{d}_8^+ \end{cases} \\ d_i^-,\ d_i^+ \geq 0,\ i = 6,7,8,9 \end{cases} \tag{22}$$

3.3. Planning Model Solving based on Optimised Particle Swarm Algorithm

In the design process of heliostat field arrangement, the positional coordinates of the absorption tower, heliostat dimensions, installation height, number of heliostats, and location of heliostats are important influencing factors affecting the optical efficiency and output efficiency of the heliostat field. The optimised particle swarm algorithm is used to solve the multi-objective linear programming equations in the case of unknown design parameters of the heliostat field.

In the three-dimensional search space, there exists a swarm of N particles, and any heliostat can be regarded as each velocity vector V_{iD} with the flight direction and velocity magnitude and the current position vector X_{iD} . All the heliostat position parameter information belongs to a feasible solution of the multivariate linear programming, which is combined with the multilevel objective function to calculate the maximum annual average output thermal power of heliostat mirrors per unit surface area under the rated annual average output thermal power of 60 MW/year. area of the heliostat is the largest annual average thermal power output.

V_{iD}, X_{iD} is updated iteratively to solve the linear optimal solution by the following equation [11]:

$$V_{iD}^{k+1} = \omega V_{iD}^{k} + c_1 r_1 (Pbest_{iD}^{k} - X_{iD}^{k}) + c_2 r^2 (Gbest_{iD}^{k}) \quad (23)$$

$$X_{iD}^{k+1} = X_{iD}^{k} + V_{iD}^{k+1} \quad (24)$$

Where V_{iD}^{k} is the velocity vector in the $D = 3rd$ dimension direction at the kth iteration of the fixed heliograph variable parameter particle i; X_{iD}^{k} is the position vector in the $D = 3rd$ dimension direction at the kth iteration of particle i; $Pbest_{iD}^{k}$ is the individual extreme value of particle i after the kth iteration; is the global optimum of particles in the population after the kth iteration; ω is the inertia weight, which indicates the particle's previous generation flight speed on the current flight speed, used to regulate the search ability of the solution space. c_1, c_2 are learning factors are taken as constant 2; r_1, r_2 are random numbers, taking the value range [0, 1].

Calculating the optimal layout scheme for unknown mirror parameters in the heliostat field, each heliostat mirror layout scheme can be regarded as a particle, and multiple heliostat mirror layout schemes constitute a particle swarm. The total number of fixed-sun mirror field is N, and the particle dimension is 3 N. The planning model solution process of the optimised particle swarm algorithm is as follows:

Step1: Set the initial state of the particle swarm according to the variable parameters of the heliostat;

Step2: Determine the initialised variable parameter position, calculate the adaptation degree of parameter particles at k iterations, and set the judging score standard;

Step3: Calculate the variable parameter objective function value, update the individual optimal solution of the particle and the population global optimal solution;

Step4: Combine equations to update the variable parameter particle velocity and position;

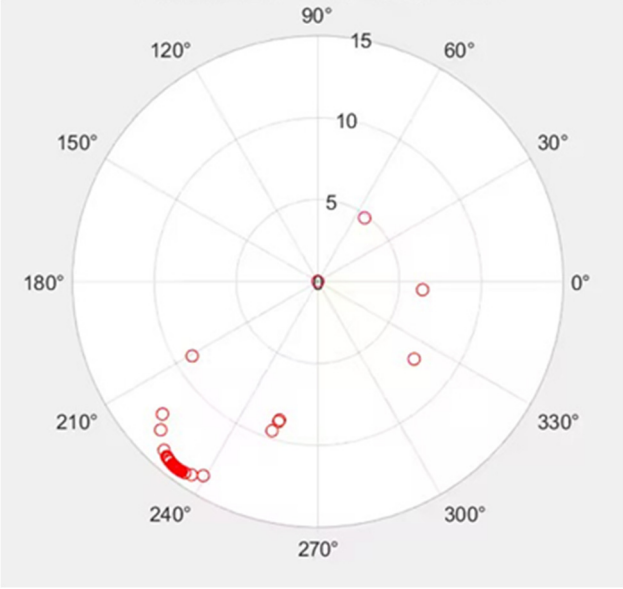

Figure 6. Global diagram of the planning model solution for the optimised particle swarm algorithm

Step5: Judge whether the current maximum number of iterations is reached or the convergence condition is satisfied, if yes, end the iteration and output the global optimal particle and its fitness value, otherwise return to Step2 to continue the iteration.

In the process of finding the optimal variable parameters, with the maximum annual average output thermal power per unit mirror area as the objective function, the speed of the programme change is controlled by updating the speed of the particles; the position of the particles is transformed by updating the position information of the fixed-sun mirrors in the programme; and searching for the maximum annual average output thermal power per unit mirror area programme.

4. Conclusion

This paper establishes a theoretical efficiency model for shadow blocking, a method for quantitatively evaluating the efficiency of shadow blocking, which can be used to predict the power loss caused by shadows. The model is based on physical principles and optical theory, which can provide a reasonable theoretical basis, and through the established model, it can provide an in-depth understanding of the mechanism of shadow influence on the performance of light energy conversion equipment, which can guide the related engineering practice; this helps to design and optimize the layout and parameters of light energy conversion equipment, so as to improve the overall efficiency of the system.

References

[1] Shi, Zhipeng. A study on the effect of dust accumulation on the reflectivity of heliostat mirrors and design of mirror dedusting device[D] Lanzhou University of Science and Technology, 2019.

[2] Du Yuhang et al, Impact analysis of different focusing strategies of heliostats in tower-type photovoltaic power plants[J], Journal of Power Engineering, 2020.40(5):426-432.

[3] Wei Bobin, Kong Lingang, Jiang Qingan et al. Simulation and experimental study of fine multitube CPC linear Fresnel concentrator system[J]. Advances in Lasers and Optoelectronics, 2019,56(03):66-73.

[4] Guo Su, Liu Deyou. Calculation of effective utilization rate of heliostat considering the shadow of receiving tower[J]. Journal of Solar Energy,2007(11):1182-1187.

[5] Duffy JA, Beckman W A (authored), Ge XS, et al (translated). Solar-thermal energy conversion process [M]. Beijing: Science Publishing, 1980.

[6] Cheng Xiaolong. Research on optimal design of tower power plant mirror field layout based on optical efficiency[D]. Hefei University of Technology,2018.

[7] Collado F.J. One-point fitting of the flux density produced by a heliostat [J]. Solar Energy,2010, 84(4): 673-684.

[8] Schwarzbozl P, Schmitz M., Pitz-Paal R. Visual HFCAL - a software for layout and optimization of heliostat fields [J]. SolarPACES, 2009.

[9] O. Farges, J.J. Bezian, M. El Hafi, Global optimization of solar power tower systems using a Monte Carlo algorithm: Application to a redesign of the PS10 solar thermal power plant [J], Renewable Energy, 2018, 119:345-353.